# Design and Testing of a CubeSat Based Deployable Robotic Arm for Small Satellites Servicing and Debris Removal Applications

IAC-25- C2,IP,48,x100293

# Design and Testing of a CubeSat Based Deployable Robotic Arm with an Electro-adhesive Gripper for Small Satellites Servicing and Debris Removal Applications

**Davide Sorli[a]*, Martina Ferrauto[a], Riccardo Mazzotti[b,f], Andrea Porceddu[c], Matteo Melchiorre[a], Lorenzo Agostini[b,f], Joseph Toma[d], Umar Farooq[e], Rocco Vertechy[b,f] and Stefano Mauro[a]**

[a] *Department of Mechanical and Aerospace Engineering, Politecnico di Torino, 10129, Italy*
[b] *Department of Mechanical Engineering, University of Bologna, 40126, Italy*
[c] *Microla Optoelectronics srl, 10144, Italy*
[d] *Axist srl, 10098, Italy*
[e] *Department of Applied Science and Technology, Politecnico di Torino, 10129, Italy*
[f] *Adaptronics srl, 20121, Italy*
* Corresponding Author

**Abstract**

This work presents the CubEArm, a novel 3U CubeSat with manipulation capabilities for on orbit servicing and debris removal, developed by Politecnico di Torino, Adaptronics and Axist . While conventional space manipulators traditionally rely on standardized interfaces such as the Launch Adapter Ring (LAR) for effective grasping, the space environment presents a significant challenge when dealing with debris or defunct satellites that may lack these predetermined features. The core innovation of the CubEArm is its novel gripper, designed and manufactured by Adaptronics and based on electro-adhesive principle of operation. This represents a significant advancement over traditional grappling mechanisms by eliminating the need for moving parts while simultaneously expanding the system's operational capabilities to interact with virtually any available surface. This versatility enhances the CubeSat's potential applications in diverse space servicing scenarios. The paper provides the design and the analysis of the robotic arm subsystem, detailing the design constraints. A key driver of the design is the capability of the system to be contained in a 2U volume when stored, and its extension to perform controlled capture of the target. Actuator and link sizing is derived from an assisted design with multibody model, simulating berthing and manipulation manoeuvres, to ensure the capability of the system to achieve the required mission. To validate the design, a high-fidelity experimental model of the complete CubEArm system was constructed. Testing focused on the capture and manipulation of a non-cooperative small satellite under relevant conditions, utilizing the microgravity testing facility provided by the Department of Mechanical Engineering (DIMEAS) at Politecnico di Torino. The design and the manufacturing of the test bench model, which involves the management of pneumatic subsystem to obtain the free floating condition, is presented. Preliminary results are discussed.
**Keywords:** Cubesat; robotic arm; space debris; in orbit servicing

## 1. Introduction

The paradigm of space operations is undergoing a significant transformation, driven by a growing interest in In-Orbit Servicing (IOS), Active Debris Removal (ADR), and In-Orbit Manufacturing (IOM). This shift is evidenced by numerous pioneering missions, from early demonstrators like JAXA's ETS-VII [1] and DARPA's Orbital Express [2] to recent commercial successes such as Northrop Grumman's Mission Extension Vehicles (MEV-1, MEV-2) [3]. With a robust pipeline of future missions planned by international agencies and commercial entities, the demand for versatile and cost-effective robotic solutions in space is undeniable [4–9].

Within this landscape, CubeSats have emerged as a disruptive platform. The commercial importance of satellites under 10 kg is highlighted by the launch of over 700 such systems between 2017 and 2022 [10]. Analysis of orbiting constellations reveals that the 3U format is the most prevalent, accounting for over 64% of CubeSats [10]. This proliferation, coupled with the strategic push towards IOS and ADR, has created a pressing need to equip these compact satellites with sophisticated robotic manipulation capabilities.

One of the best-known research activities in the field of CubeSats equipped with robotic manipulators is the AMODS (Autonomous Mobile On-orbit Diagnostic System) project developed by the United States Naval Academy (USNA) with the aim of designing a CubeSat system based on two 3U CubeSats, one equipped with thrusters called BRICSat and one with manipulation capabilities called RSat [11]. One possible application is the servicing of spacecraft already in orbit (on-orbit spacecraft servicing). For this application, a mechanical design has been developed that includes two robotic arms with 7 degrees of freedom [12] that can be used to: balance the attitude during rendezvous, dock and move on the client spacecraft, and perform inspections or repairs. The launch of a first RSat prototype was planned


https://doi.org/10.52202/083088-0096

for early 2017 through a NASA initiative, but in [13] RSat is declared dead-on-arrival, without being able to test its operation in orbit.

Studies on RSat led to a second generation of robotic arms developed by the USNA, called Intelligent Space Assembly Robot (ISAR) [14], which inherits the hardware of the RSat spacecraft, combining it with an advanced autonomous robotic system for autonomous space assembly operations. The ISAR robotic manipulator has been tested on the ground [15] and integrated more effectively with vision sensors in the Robotic Experimental Construction Satellite (RECS) designed by NSTAR (Naval Academy Satellite Team for Autonomous Robotics) [13].

Among other possible space assembly missions for small satellites, those planned for the assembly of Asteroid Redirect Vehicles, or Sun Shields, which do not require long-range manipulation capabilities, are of particular interest. In addition, technology has been developed for assembling small telescopes or scale spacecraft parts based on CubeSat satellites [14,16]. Another CubeSat prototype that demonstrates manipulation capabilities is REMORA [17], designed primarily to track existing space debris, attach itself to it and deflect its orbit in order to avoid collisions with active spacecraft. REMORA is available in two sizes, CubeSat 6U and 12U. The operation of the arm was simulated in [18] to demonstrate the feasibility of approach and grasping. [19] describes a multi-arm CubeSat for satellite maintenance operations (On-Orbit Satellite Surgery) that incorporates two robotic arms with 7 degrees of freedom each, two surgical instruments with 4 degrees of freedom, two capture arms with 3 degrees of freedom and a rigid arm with 1 degree of freedom in a 6U, 2.7 kg space. The system has been demonstrated through laboratory and telerobotics tests [20].

One of the most recent prototypes of robotic arms for CubeSats is described in [21]. The arm is designed to be stored in a 1U volume, not including the associated electronics. The arm has 3 passive degrees of freedom, which are irreversibly activated by 3 springs in order to deploy the manipulator. Under operating conditions, the arm's movement results from three active degrees of freedom, while its gripping capacity is provided by an end-effector that can also be deployed.

A further fundamental challenge lies in the end-effector technology. Conventional space-rated grippers are typically designed for cooperative targets featuring predefined grapple fixtures [22]. This approach is unsuitable for the vast majority of existing space assets and debris, which lack such features and present non-cooperative, often smooth or curved, surfaces. While passive dry adhesion inspired by gecko feet has been explored [23–25], electro adhesion presents a more promising active solution. Electro adhesive grippers offer controllable attachment and detachment, tunable holding forces, and are lightweight, compact, and energy-efficient [25–28], making them ideally suited for the power and volume constraints of a CubeSat.

To address these challenges, this paper introduces the CubEArm project: a robotic system designed for a 3U CubeSat platform to perform IOS and ADR missions. This work presents the design, development, and experimental validation of a novel system integrating a 3-degree-of-freedom robotic arm with a custom-developed Electro Adhesive (EA) gripper provided by Adaptronics [29]. The primary contribution of this paper is the demonstration of an integrated prototype, validated in a relevant laboratory environment to achieve Technology Readiness Level (TRL) 6. The following sections detail the mechatronic design of the manipulator, the principles of the electro adhesive end-effector, the system's control architecture, and the results of the experimental validation campaign.

## 2. CubEArm design

### *2.1 CubEArm requirements*

The CubEArm use case is framed within IOS/ADR mission scenarios in low Earth orbit (LEO). The device is designed to enable berthing with a target satellite and to manage the relative motion between the two satellites through its robotic arm. For the design of the CubEArm, the reference target is a mini satellite with a mass of approximately 100 kg and dimensions of 0.6 × 0.6 × 0.95 m. Its external surfaces are assumed to be composed of solar panels, aluminium, carbon fiber, or multilayer insulation (MLI). The target satellite is modeled with flat, 90-degree faces, and its specifications are inspired by the SkySat constellation.[30]

The robotic arm and its subsystems must fit within a total volume of 3U. Specifically, the arm and end-effector are allocated 2U, while the motor drivers, control board, and power supply must be contained within the remaining 1U. Each unit (1U) corresponds to a maximum mass of 2 kg, setting the overall system mass limit at 6 kg.

The payload capacity of the robotic arm is defined as 1 N, consistent with the performance of the EA gripper and the selected control strategy. A planar 3-degree-of-freedom (DOF) architecture has been adopted for the arm. This configuration satisfies project requirements regarding volume and mass constraints while providing a sufficient workspace to execute the intended maneuvers. The kinematic scheme of the manipulator is shown in Fig. 1. In Table 1 are shown the Denahvit Hartenberg (DH) parameters of the CubEArm robotic arm.



https://doi.org/10.52202/083088-0096

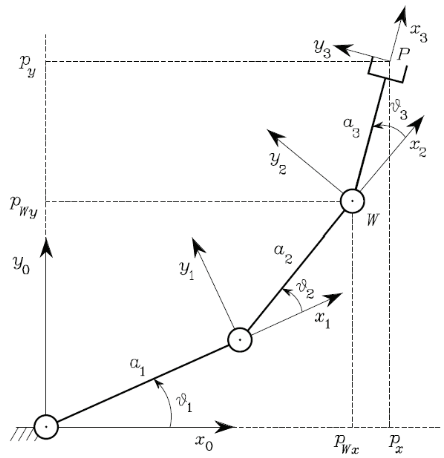


**Fig. 1. Kinematic scheme of the manipulator**

Table 1. Denahvit Hartenberg parameters of the CubEArm

| Link | $a_i$ | $\alpha_i$ | $d_i$ | $\theta_i$ |
|---|---|---|---|---|
| 1 | $a_1$ | 0 | 0 | $\theta_1$ |
| 2 | $a_2$ | 0 | 0 | $\theta_2$ |
| 3 | $a_3$ | 0 | 0 | $\theta_3$ |

*2.2 High fidelity model*

A high-fidelity model of the manoeuvre has been developed in the MATLAB/Simscape environment. The model is constructed using the rigid body modelling (RBM) approach, a well-established technique widely employed during the design phase of robotic systems of this type. [31,32]. The model includes the free-floating target satellite, the CubEArm satellite, the robotic arm, and the gripper. It supports the design process by helping define the requirements for the robotic arm joints. Once the design is finalized, the model is also used to verify compliance with project requirements in a simulated environment.

The mission scenario consists of two main phases. The first phase involves the approach and capture of the target satellite by the CubEArm, during which an impact occurs between the EA gripper and the target interface. To improve compliance in this phase, a torque control strategy is implemented on joint 2. The second phase concerns the relative handling maneuver, under the assumption of either an IOS or a deorbiting mission. The multibody model has been developed to simulate both phases.

To identify the joints' actuators requirements it is chosen a robotic arm configuration that maximize the workspace while maintaining a encumbrance. DH parameters of this configuration are shown in Table 2.

Table 2. DH parameters of the maximum workspace configuration assumed for the sizing of the actuators

| Link | $a_i$ [m] | $\alpha_i$ | $d_i$ | $\theta_i$ |
|---|---|---|---|---|
| 1 | 0.200 | 0 | 0 | $\theta_1$ |
| 2 | 0.200 | 0 | 0 | $\theta_2$ |
| 3 | 0.020 | 0 | 0 | $\theta_3$ |

The results obtained from the multibody simulation are corrected according to the safety coefficient provided by the ECSS standards [33]. In particular, for inertial loads such as in the case under consideration, a safety coefficient of 2.2 is applied to the torque measured at the joints.

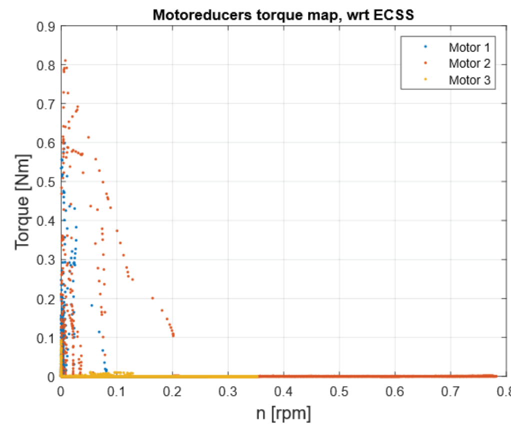


Fig. 2. Torque map required to actuators in the first phase of the manoeuvre

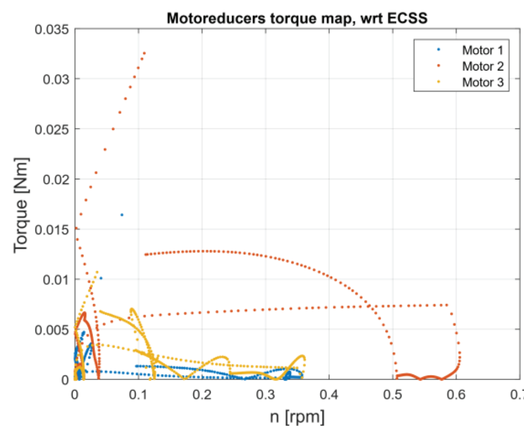


Fig. 3. Torque map required to actuators in the second phase of the manoeuvre

Fig. 2 presents the torque map required by the actuators during the first phase of the manoeuvre, while Fig. 3 shows the corresponding torque map for the second phase. Results reported in Table 3 indicate that, for all actuators, the first phase is the most critical in terms of both torque and power demand.


https://doi.org/10.52202/083088-0096

Table 3. Actuators torque and power requirements, result of the multibody simulation

| | Phase 1 | | Phase 2 | |
|---|---|---|---|---|
| | Torque [Nm] | Power [mW] | Torque [Nm] | Power [mW] |
| Actuator 1 | 0.63 | 2.2 | 0.012 | 0.3 |
| Actuator 2 | 0.83 | 8.1 | 0.032 | 0.9 |
| Actuator 3 | 0.12 | 0.2 | 0.010 | 0.2 |

### *2.3 Robotic arm design*

The actuators for the robotic arm are selected from the Maxon catalogue. For the first and second joints, the EC45 flat brushless motor is adopted, while the third joint employs the EC9.2 flat brushless motor. The chosen reducer for the first and second joints is the GS45A spur gearhead, with gear ratios of 18:1 and 61:1, respectively. For the third joint, the GP10A planetary gearhead is used, with a gear ratio of 256:1.

The selected actuators are equipped with built-in Hall sensors. However, to guarantee precise control of the CubEArm, the system is also fitted with OSRAM AS5048A absolute magnetic encoders mounted on the reducer side. This configuration allows direct measurement of the joint angular position, resulting in smoother robotic motion. The definition of the final robotic arm geometry required an iterative design process to ensure that all subsystems could be accommodated within the allocated 2U volume when the arm is fully retracted. The resulting DH parameters are shown in Table 4.

Table 4. Final DH parameters of the CubEArm

| Link | $a_i$ $[m]$ | $\alpha_i$ | $d_i$ | $\theta_i$ |
|---|---|---|---|---|
| 1 | 0.105 | 0 | 0 | $\theta_1$ |
| 2 | 0.171 | 0 | 0 | $\theta_2$ |
| 3 | 0.050 | 0 | 0 | $\theta_3$ |

The non-commercial components of the CubEArm are manufactured in PLA-CF using FDM additive manufacturing. Production is carried out with a BambuLab X1E 3D printer.

### *2.4 Electro Adhesive gripper*

The EA gripper features a two-sided, flat architecture that is arranged at 90° to itself. This architecture enables satellites with flat surfaces and 90° edges to be captured. This type of gripper provides a reliable grip for several reasons: the redundancy of the electro-adhesive elements (with two independent devices, one on each face); the ability to resist multidirectional stresses on the adhesive surfaces, particularly in the normal and tangential directions; the self-centring capacity of the gripping device; and the absence of mechanical actuation.

The gripper electronic system is composed by the following subsystems:

- MCU (microcontroller unit): the system microcontroller
- HV transformer: the driver and source for generating the high voltage required to power the EA elements
- Power supply and conditioning circuit for the capacitive sensor: for proximity and contact sensing of the object to be grasped
- Current and voltage probe: for monitoring the status and correct functioning of the EA elements

For the purposes of the project, which involves validating the CubEArm for gripping and manipulating objects in simulated gravity conditions in laboratory, it was decided to focus on commercial solutions for industrial applications, with proven reliability and flexibility in high-frequency cycle control and monitoring and high accuracy of complex systems. During testing, this electronics is placed on the auxiliary air bearing structure of the microgravity bench, but outside the CubEArm. For the grasping and manipulation tests, functional aspects (performance, reliability, versatility and redundancy) are prioritised over miniaturisation requirements.

A photo of an example of two EA grippers is shown in Fig. 4.

Fig. 4. Example of two Electro adhesive grippers

The EA gripper can be designed to allow high level of conformability for a better grip in case of initial misalignments between gripper and interface of the target. The grip is secured by the EA film (SpacEAAL, from Adaptronics), which can be folded during the flight phase and deployed once the target needs to be approached.

## 3. Testing facility

To verify that the CubEArm meets the project objectives, an experimental campaign was carried out using the microgravity testing facility of the Department



https://doi.org/10.52202/083088-0096

of Mechanical and Aerospace Engineering (DIMEAS) at the Polytechnic University of Turin. This facility is designed for testing devices equipped with air bearings, which allow them to float over the laboratory's smooth resin floor, effectively replicating planar microgravity conditions.

For laboratory testing, some modifications to the CubEArm design were necessary. In particular, an auxiliary structure was integrated to accommodate the pneumatic system required to generate the microgravity environment. The auxiliary structure is also used to house the electronic system of the gripper. In Fig. 5 it is shown the final prototype.

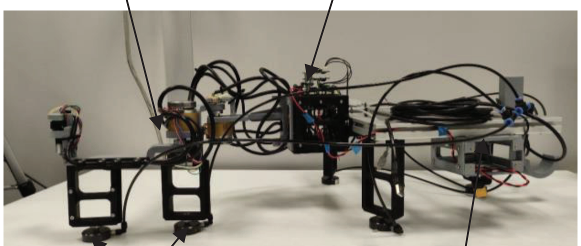


Fig. 5. CubEArm prototype used during the experimental campaign

The CubEArm mission scenario consists of three phases: approach, capture, and relative maneuvering with respect to a non-cooperative target satellite. The experimental campaign addresses only the latter two phases, while the approach maneuver is not simulated. The objective of the experiments is to validate the capability of the EA gripper to effectively capture the target satellite and to demonstrate that the designed robotic arm can perform the required maneuvers. For the present experimental campaign, an EA gripper with a passive joint was employed, allowing an initial opening between the faces greater than 90°. During the contact phase, the joint allows the closing of the gripper angle thanks to two elastic elements. This feature allows a better grip in the case of initial misalignments between gripper and interface of the target. The mission phase in which the CubEArm approaches the target using its own thrusters and GNC system has not yet been validated and will be investigated in future developments of the project.

The target satellite is represented by a structure constructed from Bosch profiles. It is equipped with three pneumatic bearings and a 2-liter, 200-bar scuba tank to supply air, enabling the target to maintain a free-floating state. Additionally, two on/off normally closed (NC) pneumatic valves, controlled via an Arduino Nano ESP32 board, allow the target to be easily switched between fixed and free-floating conditions. This feature facilitates experimental setup and ensures test repeatability. The gripper interface is mounted on one side of the target, enabling evaluation of the gripper's effectiveness on various surface materials.

Since the CubEArm is not equipped with its own GNC system, the experimental facility requires a device to impose the initial approach velocity. This was achieved by employing a UR5 robotic manipulator, fixed to the laboratory floor. The UR5 holds the CubEArm using a gripper, which can move it with a controlled and repeatable velocity. When the CubEArm approaches sufficiently close to the target interface, a screen mounted on the CubEArm gripper triggers a photocell sensor on the target. The photocell signal is used to actuate the pneumatic valves on the target and to command the UR5 gripper to release the CubEArm. This signal simultaneously marks the official start of the experiment.

The experimental setup is shown in Fig. 6.

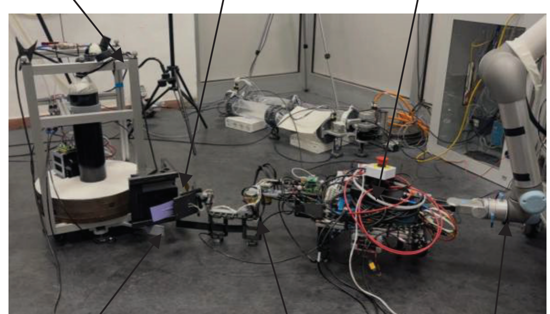


Fig. 6. CubEArm experimental setup

**4. Results**

The test consists in two critical phases: in the first phase the robotic arm and the EA gripper must be able to capture and secure the target satellite. In the second phase the robotic arm must be able to modify the CubEArm attitude with respect to the target. The sequence of the manoeuvre is shown in Fig. 7

Fig. 7.a. shows the initial condition of the experiment. The CubEArm is launched by the UR5 and the EA gripper contacts with the free floating target. The gripper demonstrates its capability to capture the target interface (MLI), and the robotic arm effectively dampen the contact, Fig. 7.b: this is the starting configuration for the operating of the robotic arm in position control. The


https://doi.org/10.52202/083088-0096

robotic arm demonstrates the capability to modify the pose of the CubEArm with respect to the target, reaching the project objective to develop a system able to perform an IOS mission. The final configuration is shown in Fig. 7.c.

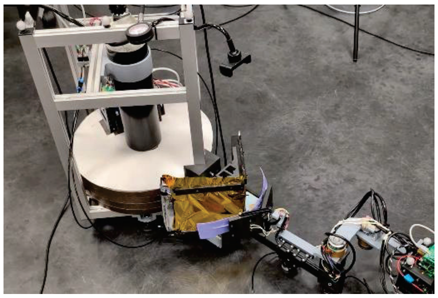

(a)

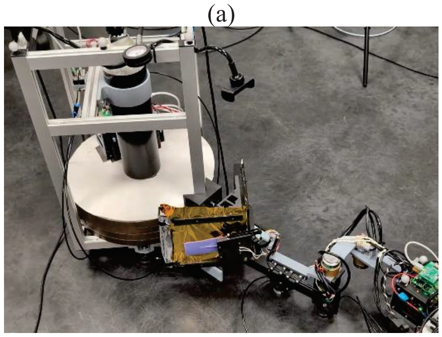

(b)

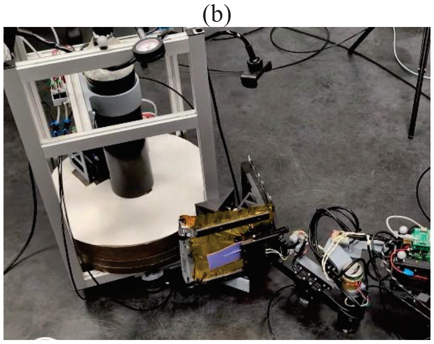

(c)

Fig. 7. Sequence of the CubEArm berthing manoeuvre.

During the acquisition of sensor data from the robotic arm, two maneuvers are performed. The first maneuver, referred to as the “Home position” in the following plots, is executed by directly providing the robotic arm controller with the joint angles corresponding to a home configuration. This configuration ensures that the arm avoids singularities during subsequent maneuvers and serves as the starting point for all tests. This phase represents the initial deployment of the robotic arm. In the second phase, called “Robot Control” in the plots, the arm is controlled in the workspace using position control, while direct kinematics is employed to determine the corresponding joint positions. This phase is the significant portion of the plots, as it represents the actual testing of the robotic arm’s control performance.

Fig. 8 presents shown the set and the feedback of the joints position. It can noted that the first and the second joint reach successfully the set position after a transient phase, while the third joint position drift. This beahviour is due an underestimation in the design phase of the uncertainties introduced by the non perfect planarity and smoothness of the resin floor, which cause unexpected external forces. In fact, the third actuator, the third link and the mechanic connection are undersized. Moreover, the EA gripper weight was underestimated in the design phase and was not foreseen to sustain it with an air bearing, causing an unexpected flession of the third link.

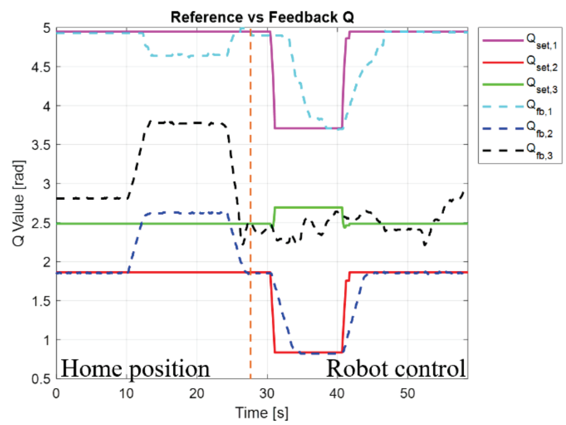


Fig. 8. Joints angular position.

Fig. 9 shows the set and feedback of the end effector position in the workspace. The trend of the plot is coherent with the joints angular position plot. Fig. 10 shows the end effector position error in the workspace. It can be observed that, after the transient phase, the error remains low, gradually drifting in correspondence with the drift of joint 3.

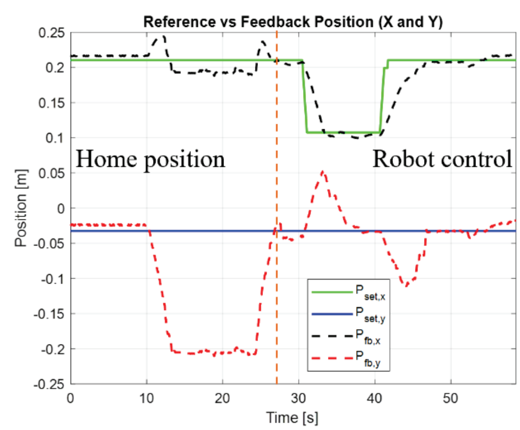


Fig. 9. End effector position in the robot workspace.



https://doi.org/10.52202/083088-0096

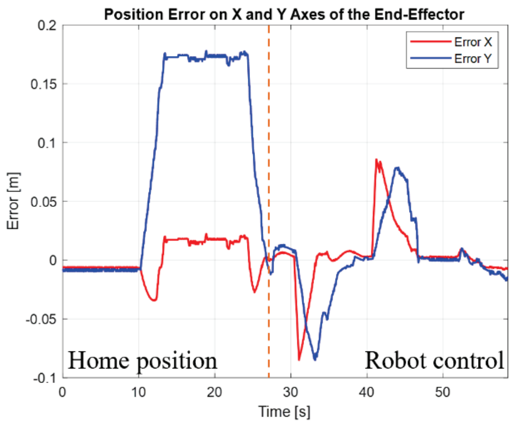


Fig. 10. End effector error in the robot workspace

## 6. Conclusions

This paper presents the design of a CubeSat-based robotic arm equipped with an electro-adhesive gripper. The use case considered is an in-orbit servicing (IOS) and inspection mission scenario. Project constraints are outlined, and the workflow followed to develop a design capable of meeting these requirements is discussed.

To validate the design, the microgravity testing facility employed is described, along with the modifications applied to the CubEArm to enable experimental testing. Experimental results demonstrate the system's ability to meet the project objectives: the gripper successfully captures the target, maintaining a firm hold during robotic arm manoeuvres, while the arm itself performs berthing operations with low positioning errors.

Future work includes a revision of the design to address limitations identified during experimental testing and the integration of a CubEArm GNC system to enable autonomous approach manoeuvres.


## Acknowledgements

This publication is part of the project CubEArm which has received funding from Cascade funding calls of NODES Program, supported by the MUR - M4C2 1.5 of PNRR funded by the European Union - NextGenerationEU (Grant agreement n. ECS00000036)


## References


[1] Oda, M., Kibe, K., and Yamagata, F., "ETS-VII, Space Robot in-Orbit Experiment Satellite," *Proceedings of IEEE International Conference on Robotics and Automation*, IEEE, pp. 739–744. https://doi.org/10.1109/ROBOT.1996.503862.

[2] Friend, R. B., 2008, "Orbital Express Program Summary and Mission Overview," R.T. Howard, and P. Motaghedi, eds., p. 695803. https://doi.org/10.1117/12.783792.

[3] Northrop Grumman, "MEV Mission." [Online]. Available: https://www.northropgrumman.com/space/space-logistics-services. [Accessed: 04-Sep-2025].

[4] Biesbroek, R., Aziz, S., Wolahan, A., Cipolla, S., Richard-Noca, M., and Piguet, L., *THE CLEARSPACE-1 MISSION: ESA AND CLEARSPACE TEAM UP TO REMOVE DEBRIS*. [Online]. Available: https://clearspace.today/.

[5] Saplan, A., "Robotic Servicing of Geosynchronous Satellites (RSGS)." [Online]. Available: https://www.darpa.mil/program/robotic-servicing-of-geosynchronous-satellites. [Accessed: 04-Sep-2025].

[6] NASA, "OSAM-1 Mission," https://www.nasa.gov/mission/on-orbit-servicing-assembly-and-manufacturing-1/.

[7] NASA, "OSAM-2 Mission," https://www.nasa.gov/mission/on-orbit-servicing-assembly-and-manufacturing-2-osam-2/.

[8] Palmieri, P., Gaidano, M., Melchiorre, M., Salamina, L., Sorli, D., Troise, M., and Mauro, S., 2024, "A Deployable and Retractable Inflatable Link for a Space Robotic Manipulator," *IAF Materials and Structures Symposium*, International Astronautical Federation (IAF), Paris, France, pp. 1517–1526. https://doi.org/10.52202/078369-0164.

[9] Palmieri, P., Gaidano, M., Troise, M., Salamina, L., Melchiorre, M., and Mauro, S., 2024, "IDRA: A Concept for an Inflatable and Retractable Robotic Arm for ISAM," *2024 11th International Workshop on Metrology for AeroSpace (MetroAeroSpace)*, IEEE, pp. 284–289. https://doi.org/10.1109/MetroAeroSpace61015.2024.10591537.

[10] Union of Concerned Scientists, "UCS Satellite Database." [Online]. Available: https://www.ucsusa.org/resources/satellite-database. [Accessed: 04-Sep-2025].

[11] Hanlon, E. A. S., Lange, M. E., Keegan, B. P., Culton, E. A., Corbett, M. J., Roser, J. G., Safbom, C. P., Wenger, B. A., and Kang, J. S., 2016, "AMODS: Autonomous Mobile on-Orbit Diagnostic System," *2016 IEEE Aerospace Conference*, IEEE, pp. 1–10. https://doi.org/10.1109/AERO.2016.7500512.

[12] Wenberg, D. L., Keegan, B. P., Lange, M. E., Hanlon, E. A. S., and Kang, J. S., 2016, "RSat Flight Qualification and Test Results for Manipulable Robotic Appendages Installed on

3u Cubesat Platform," *30th Annual AIAA/USU Conference on Small Satellites*, pp. 1–9.

[13] Knight, A. N., Tetterton, T. R., Engl, A. J., Sinkovitz, P. M., Ward, B. J., and Kang, J. S., 2020, "Design and Development of On-Orbit Servicing CubeSat-Class Satellite," *34th Annual Small Satellite Conference*.

[14] Gregory, J. M., Kang, J. S., Sanders, M., Wenberg, D., and Sega, R. M., 2019, "Characterization of Semi-Autonomous On-Orbit Assembly CubeSat Constellation," *33rd Annual AIAA/USU Conference on Small Satellites*.

[15] Wenberg, D. L., Hanlon, E. A., Rubiocastaneda, B., Lai, T., and Kang, J., 2017, "Intelligent Space Assembly Robot: Design and Ground Testing," *AIAA SPACE and Astronautics Forum and Exposition*, American Institute of Aeronautics and Astronautics, Reston, Virginia. https://doi.org/10.2514/6.2017-5180.

[16] Underwood, C., and Pellegrino, S., 2011, "Autonomous Assembly of a Reconfigurable Space Tele-Scope (AAReST) for Astronomy and Earth Observation," *8th IAA Symposium on Small Satellites for Earth Observation, Berlin*.

[17] McCormick, R., Austin, A., Wehage, K., Backus, S., Miller, R., Leith, J., Bradley, B., Durham, P., and Mukherjee, R., 2018, "REMORA CubeSat for Large Debris Rendezvous, Attachment, Tracking, and Collision Avoidance," *2018 IEEE Aerospace Conference*, IEEE, pp. 1–13. https://doi.org/10.1109/AERO.2018.8396814.

[18] Setterfield, T. P., McCormick, R., Kim, J., and Mukherjee, R., 2020, "Multibody Simulation of REMORA CubeSat Docking to and Pushing a Spent Rocket Booster," *2020 IEEE Aerospace Conference*, IEEE, pp. 1–12. https://doi.org/10.1109/AERO47225.2020.9172500.

[19] Nye, T., Schurr, A., and Milam, M., 2019, "Development of a MicroSat for On-Orbit Satellite Surgery," *33rd Annual AIAA/USU Conference on Small Satellites*.

[20] Nye, T., and Milam, M., 2020, "Advancements of a MicroSat for On-Orbit Satellite Surgery," *34th Annual Small Satellite Conference*.

[21] Liu, J., Zhao, P., Chen, K., Zhang, X., and Zhang, X., 2022, "1U-Sized Deployable Space Manipulator for Future On-Orbit Servicing, Assembly, and Manufacturing," Space: Science & Technology, **2022**. https://doi.org/10.34133/2022/9894604.

[22] Whelan, D. A., Adler, E. A., Wilson III, S. B., and Roesler, Jr. , G. M., 2000, "DARPA Orbital Express Program: Effecting a Revolution in Space-Based Systems," B.J. Horais, and R.J. Twiggs, eds., pp. 48–56. https://doi.org/10.1117/12.406656.

[23] Purtov, J., Frensemeier, M., and Kroner, E., 2015, "Switchable Adhesion in Vacuum Using Bio-Inspired Dry Adhesives," ACS Appl Mater Interfaces, **7**(43), pp. 24127–24135. https://doi.org/10.1021/acsami.5b07287.

[24] Estrada, M. A., Hockman, B., Bylard, A., Hawkes, E. W., Cutkosky, M. R., and Pavone, M., 2016, "Free-Flyer Acquisition of Spinning Objects with Gecko-Inspired Adhesives," *2016 IEEE International Conference on Robotics and Automation (ICRA)*, IEEE, pp. 4907–4913. https://doi.org/10.1109/ICRA.2016.7487696.

[25] Jiang, H., Hawkes, E. W., Arutyunov, V., Tims, J., Fuller, C., King, J. P., Seubert, C., Chang, H. L., Parness, A., and Cutkosky, M. R., 2015, "Scaling Controllable Adhesives to Grapple Floating Objects in Space," *2015 IEEE International Conference on Robotics and Automation (ICRA)*, IEEE, pp. 2828–2835. https://doi.org/10.1109/ICRA.2015.7139584.

[26] Krape, R. P., 1968, *Applications Study of Electroadhesive Devices*.

[27] Ritter, M., and Barnhart, D., 2017, "Geometry Characterization of Electroadhesion Samples for Spacecraft Docking Application," *2017 IEEE Aerospace Conference*, IEEE, pp. 1–8. https://doi.org/10.1109/AERO.2017.7943683.

[28] Guo, J., Leng, J., and Rossiter, J., 2020, "Electroadhesion Technologies for Robotics: A Comprehensive Review," IEEE Transactions on Robotics, **36**(2), pp. 313–327. https://doi.org/10.1109/TRO.2019.2956869.

[29] Carloni, A., Valori, M., Bertolucci, F., Agostini, L., Berselli, G., Fassi, I., Tosatti, L. M., and Vertechy, R., 2025, "Enhancing Compliant Gripper Performance: Exploiting Electro-Adhesion to Increase Lifting Force over Grasping Force," Robot Comput Integr Manuf, **91**, p. 102843. https://doi.org/10.1016/j.rcim.2024.102843.

[30] ESA, "SkySat." [Online]. Available: https://earth.esa.int/eogateway/missions/skysat. [Accessed: 04-Sep-2025].

[31] Sorli, D., Ferrauto, M., Melchiorre, M., Palmieri, P., Salamina, L., and Mauro, S., 2024, "A Simulation Tool to Evaluate Different Capture Strategies in a Berthing Maneuver," *Volume 5: Dynamics, Vibration, and Control*, American Society of Mechanical Engineers. https://doi.org/10.1115/IMECE2024-144113.

[32] Palmieri, P., Troise, M., Salamina, L., Gaidano, M., Melchiorre, M., and Mauro, S., 2023, "An Inflatable 7-DOF Space Robotic Arm for Active



https://doi.org/10.52202/083088-0096

Debris Removal," pp. 580–589. https://doi.org/10.1007/978-3-031-45770-8_58.

[33] European Cooperation for Space Standardization, 2019, *ECSS-E-ST-33-01C Rev.2 – Mechanisms*.

-